UDK 621.454.2 https://doi.org/10.15407/itm2025.04.019

O. S. CHERNIAVSKYI[1], S. I. DOLGOPOLOV[2], S. A. SHEVCHENKO[3]

MODELING OF A CHECK VALVE OPERATION IN THE RECONFIGURABLE HYDRAULIC FEED SYSTEM OF A LIQUID ROCKET ENGINE

[1] Oles Honchar Dnipro National University, 72 Nauky Avenue, Dnipro, 49045 Ukraine; e-mail: o.s.cherniavskyi@gmail.com
[2]Institute of Technical Mechanics of the National Academy of Sciences of Ukraine and State Space Agency of Ukraine, 15 Leshko-Popelya Str., Dnipro, 49005 Ukraine; e-mail: dolmrut@gmail.com
[3] Institute of Transport Systems and Technologies of the National Academy of Sciences of Ukraine, 5 Pisarzhevsky Str., Dnipro, 49005 Ukraine; e-mail: sergiishevch@gmail.com

Серед різноманіття агрегатів автоматики пневмогідравлічних систем ракетної техніки широке застосування знайшли зворотні клапани. Найчастіше їх використовують у лініях заправлення різних ємностей, у магістралях наддуву паливних баків ракет-носіїв, де вони запобігають зворотному потоку та проникненню парів у системи наддуву. У рідинних ракетних двигунах (РРД) зворотні клапани встановлюють у дренажних лініях та в лініях продування інертними газами. Окрему увагу заслуговує використання зворотних клапанів у гідравлічних системах змінної структури, у яких під час роботи РРД відбувається зміна напрямків потоків рідини. Метою роботи є розроблення математичної моделі динамічних процесів у зворотному клапані, верифікованої за результатами CFD–розрахунків розподілу тиску на поверхні тарілки запірного органу, та застосування цієї моделі для аналізу перехідних процесів у гідравлічній системі змінної структури. Для визначення сили дії потоку на тарілку клапана запропоновано підхід у наближенні із зосередженими параметрами, який ґрунтується на балансі витрат робочої рідини у проточній частині клапана. Розглянуто потік у радіальному напрямку на вході клапана, який залежить від ходу тарілки, та потік на периферії запірного органу, у вузькій щілині між корпусом і тарілкою. Для реалізації цього підходу достатньо знати геометричні характеристики клапана та значення коефіцієнтів витрати, які приймаються постійними. Для гідравлічної системи живлення пальним змінної структури, що містить зворотні клапани, розроблено математичну модель низькочастотних динамічних процесів і виконано розрахунки перехідних процесів під час запуску РРД. У процесі запуску двигуна живлення пальним його газогенератора автоматично перемикається за допомогою зворотних клапанів: живлення від пускового бачка змінюється на живлення від насоса. Розрахунки перехідних процесів виконано для двох варіантів завдання сили дії потоку на тарілку зворотного клапана: за результатами CFD–аналізу та за наближенням із зосередженими параметрами. Показано задовільну узгодженість результатів цих розрахунків. Обґрунтовано можливість використання запропонованого наближення із зосередженими параметрами для визначення сили дії потоку на тарілку зворотного клапана для побудови математичних моделей динамічних процесів у гідравлічних системах змінної структури без залучення трудомістких CFD–розрахунків.

Ключові слова: *рідинний ракетний двигун, система живлення змінної структури, зворотний клапан, математичне моделювання, CFD-аналіз, сила дії потоку рідини, запуск двигуна*.

Among the various automation units used in pneumatic–hydraulic systems of rocket hardware, check valves are widely employed. They are most commonly used in the filling lines of different tanks and in the pressurization lines of launch vehicle propellant tanks, where they prevent reverse flow and the ingress of vapors into the pressurization system. In liquid rocket engines (LREs), check valves are installed in drainage lines and in inert gas purging circuits. Particular attention is given to the use of check valves in reconfigurable hydraulic systems, in which the flow direction changes during the LRE operation. The goal of this study is to develop a mathematical model of dynamic processes in a check valve, verify it using CFD simulations of the pressure distribution over the valve poppet surface, and apply it to the analysis of transient processes in a reconfigurable hydraulic system. To determine the flow force acting on the valve poppet, this paper proposes an approach in the lumped-parameter approximation based on the flow rate balance of the working fluid in the valve flow passage. The model considers the radial inflow at the valve inlet, which depends on the poppet travel, and the peripheral flow through the narrow clearance between the valve body and the poppet. To implement this approach, it is sufficient to know the valve geometry and the discharge coefficients, which are assumed to be constant. For a reconfigurable propellant feed system containing check valves, a mathematical model of low-frequency dynamic processes was developed, and transient processes during the LRE startup were simulated. During the startup, the propellant feed of the LRE gas generator is automatically switched by the check valves from the start tank supply to the pump supply. Transient processes were simulated for the flow force acting on the check valve poppet determined using CFD simulation and the lumped-parameter approximation. A satisfactory agreement between the results of these two ap-

proaches was demonstrated. The possibility of using the proposed lumped-parameter approximation to determine the flow force acting on the check valve poppet was justified, thus enabling the development of mathematical models of dynamic processes in reconfigurable hydraulic systems without resorting to computationally expensive CFD simulations.

Keywords*: liquid rocket engine, branched reconfigurable feed system, check valve, mathematical modeling, CFD analysis, fluid flow force, engine startup*.

Introduction. Among the wide range of automation units in pneumatic–hydraulic systems of rocket technology, check valves are widely used. They are most often installed in filling lines of various tanks and in pressurization lines of launch-vehicle propellant tanks, where they prevent reverse flow and the ingress of vapors into the pressurization system [1]. In liquid propellant rocket engines (LPREs), check valves are installed in the lines that deliver liquid and gaseous propellant components, as well as in drain lines, to ensure reliable isolation between the oxidizer and fuel circuits. In reusable start LPRE systems of upper stages and spacecraft, they are placed in inert gas purge lines between engine duty cycles [2].

The use of check valves in variable-structure hydraulic systems merits special attention [3]. In such systems the direction of liquid flow changes during LPRE operation. A representative example is the fuel feed system in staged-combustion LPRE cycles [4, 5], where ignition of the propellant components is accomplished using a starting fuel. After engine start and transition to steady operation, the feed switches over to the main fuel.

Reliable prediction of LPRE start up performance requires validated mathematical models of the dynamic processes in the engine systems and units. In staged-combustion LPREs, modeling the flow direction reversal and the dynamics of check valve operation is of particular importance.

A number of recent papers have addressed check valve operation [6 – 8]. They consider various aspects: design and improvement of structures, methods to reduce hydraulic resistance [6], and determination of static and dynamic characteristics [7, 9]. Various approaches have been examined for modeling the dynamics of direct acting safety valves with a poppet closure member [10 – 13].

To tackle these problems, many researchers employ CFD analysis [6–8, 10–15]. For example, [6] performed CFD modeling of a poppet type check valve in ANSYS Fluent to select an adequate turbulence model for accurate prediction of hydraulic losses. Paper [7] focuses on improving the discharge characteristics of an adjustable check valve and reducing pressure losses. The dependence of the valve flow coefficient on the working fluid volumetric flow rate was established. The authors of [10] highlight two principal CFD approaches for modeling flow forces in hydraulic valves. The first fixes the position of the moving part (no motion), used in both steady and unsteady regimes. The second accounts for motion of the closure member under flow action and is implemented via FSI modeling (fluid–structure interaction), which tracks fluid–solid interaction. The first approach is used in [11, 12] to evaluate force distribution over a safety valve poppet. An example of the FSI approach is [13], where user defined functions update the poppet position at each time step based on flow and spring forces. Study [14] describes direct and indirect methods of CFD modeling for a poppet type safety valve. Boundary conditions were inlet and outlet pressures: in the direct method the outlet pressure is kept constant, while in the indirect method both inlet and outlet pressures are varied. The authors of [15] developed a CFD model of a poppet valve that reproduces its behavior in both steady and transient regimes. Pressure and flow rate were prescribed for steady runs and fixed pressure for transients.

Although FSI models reproduce valve dynamics with high fidelity, they are computationally expensive. In large hydraulic systems where a check valve is only one of many components their use is constrained. Lumped parameter models are widely used in such cases. They capture system dynamics with far lower

computational cost. A combined approach is the most rational: local hydrodynamic effects (pressure forces, flow coefficients, etc.) are obtained from CFD, while the overall system dynamics are computed using a lumped parameter model. This approach is implemented, for example, in [8], which investigated hydrodynamic effects leading to undesirable water hammer in pipeline systems. The present work adopts a similar combined approach.

The objective of this work is to develop a mathematical model of the dynamic processes in a check valve, verified against CFD results for the pressure distribution over the poppet surface, and to apply this model to analyze transients in a variable structure hydraulic system.

Reconfigurable fuel feed hydraulic system. The objects of study are check valves in the fuel feed hydraulic system of a reusable start LPRE. Ignition of the propellant components is provided by gas-dynamic igniters [16, 17]. Their operating principle relies on the Hartmann–Sprenger effect [18]. A fragment of the computational scheme of the variable structure fuel feed system under study is shown in Fig. 1. The scheme includes feed lines connecting the gas generator, starting tank, fuel pump, and two check valves. At the initial stage of start, fuel is delivered to the gas generator from the starting tank. After ignition in the gas generator the turbopump shaft spins up, the fuel pump builds high pressure, and the check valves close off the flow from the starting tank and open the pump feed.

The check valves are identical in design and characteristics. Their computational scheme is given in Fig. 2. To reduce the region of unstable valve behavior during engine start the radial clearance between the poppet and the body has a minimal area. This design feature increases the flow force acting on the poppet from the inlet side even at small clearances between the poppet and the seat. In addition, the inlet nozzle diameter is smaller than the seat diameter. This must be accounted for in valve hydrodynamics because the flow turns before entering the annular clearance between the poppet and the seat.

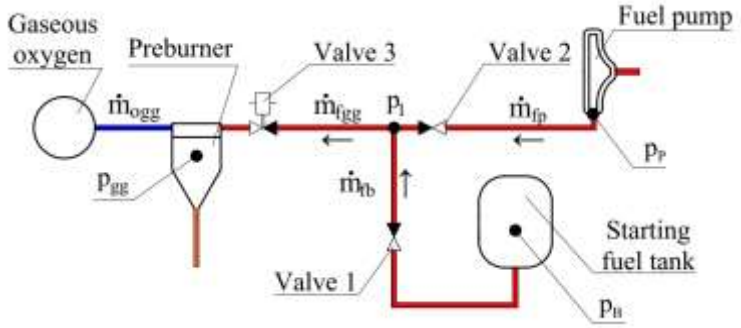

$\dot{m}_{ogg}$ – oxidizer flow rate to the gas generator; $\dot{m}_{fgg}, \dot{m}_{fb}, \dot{m}_{fp}$ – fuel flow rates in the respective branches; p_1 – pressure at the branching node; p_{gg} – gas generator pressure; p_B – starting tank pressure; p_P – fuel pump discharge pressure

Fig. 1 – Schematic of the gas generator fuel feed system

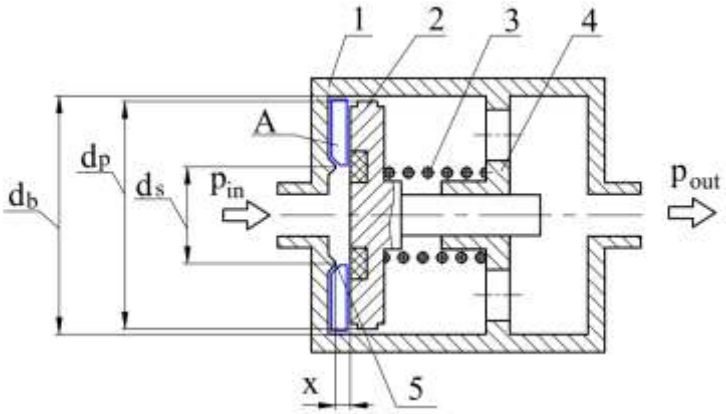

1 – body; 2 – poppet; 3 – spring; 4 – baffle; 5 – seat;
d_s – seat diameter; d_b – inner body diameter;
d_p – poppet diameter; p_{in}, p_{out} – fluid pressures at the valve inlet and outlet

Fig. 2 – Schematic of the check valve

Mathematical model of the dynamics of the reconfigurable feed system. The low frequency mathematical model of the gas generator feed system under study (see Fig. 1) comprises: a lumped parameter model of the hydraulic lines, an equation for the gas generator pressure, and equations of motion for the check valve closure members. To build the dynamics model of the hydraulic lines, we used an approach developed for extended, branched pipelines [4, 5]. First, the frequency responses of the different branches of the hydraulic system are obtained by the impedance method for a distributed parameter system. Next, a lumped parameter model is assembled whose coefficients are chosen so that the frequency responses of the distributed and lumped models agree within a specified accuracy over the target frequency band.

Following this approach, the nonlinear lumped parameter model of the dynamics of the variable structure fuel feed hydraulic system takes the form of equations (1) – (5)

$$J_{\text{fp}} \frac{d\dot{m}_{\text{fp}}}{dt} = p_{\text{p}} - p_1 - \left(\xi_{\text{fp}} + \xi_{\text{V2}}\right) \Big/ \rho \cdot \dot{m}_{\text{fp}}^2 , \tag{1}$$

$$J_{\text{fb}} \frac{d\dot{m}_{\text{fb}}}{dt} = p_{\text{b}} - p_1 - \left(\xi_{\text{fb}} + \xi_{\text{V1}}\right) \Big/ \rho \cdot \dot{m}_{\text{fb}}^2 , \tag{2}$$

$$C_1 \frac{dp_1}{dt} = \dot{m}_{\text{fp}} + \dot{m}_{\text{fb}} - \dot{m}_{\text{fgg}} , \tag{3}$$

$$J_{\text{fgg}} \frac{d\dot{m}_{\text{fgg}}}{dt} = p_1 - p_{\text{gg}} - \left(\xi_{\text{fgg}} + \xi_{\text{V3}}\right) \Big/ \rho \cdot \dot{m}_{\text{fgg}}^2 , \tag{4}$$

$$\frac{V_{\text{gg}}}{\gamma_{\text{gg}} R_{\text{gg}} T_{\text{gg}}} \frac{dp_{\text{gg}}}{dt} = \dot{m}_{\text{ogg}} + \dot{m}_{\text{fgg}} - \dot{m}_{\text{sgg}} , \tag{5}$$

$$\dot{m}_{\mathrm{sgg}} = \frac{A_{\mathrm{gg}} p_{\mathrm{gg}}}{\sqrt{R_{\mathrm{gg}} T_{\mathrm{gg}}}} \sqrt{\gamma_{\mathrm{gg}} \left(\frac{2}{\gamma_{\mathrm{gg}} + 1} \right)^{\frac{\gamma_{\mathrm{gg}}+1}{\gamma_{\mathrm{gg}}-1}}},$$

here ρ – is the fuel density; $\dot{m}_{\mathrm{ogg}}$ – is the oxidizer flow rate supplied to the gas generator; $\dot{m}_{\mathrm{sgg}}$ – is the mass flow rate of combustion products leaving the gas generator; ξ_{fp}, ξ_{fb}, ξ_{fgg} – are hydraulic resistance coefficients obtained from hydraulic calculation; J_{fp}, J_{fb}, J_{fgg} – are inertial resistance coefficients determined from the pipeline geometry; ξ_{V1}, ξ_{V2}, ξ_{V3} – are hydraulic resistance coefficients of the check valves determined by their effective flow areas; V_{gg} is volume of the combustion chambers in the preburner; R_{gg} is specific gas constants of the combustion products in the preburner; T_{gg} is temperature of the combustion products in the preburner; γ_{gg} is adiabatic indice (ratios of specific heats) of the combustion products in the preburner; A_{gg} is critical nozzle throat area of the preburner; C_1 is concentrated compliance.

The motion of each check valve poppet is governed by the equation of motion:

$$m_{\mathrm{ms}} \frac{d^2 x}{dt^2} = F_{\mathrm{flow}} - F_{\mathrm{sp}}, \tag{6}$$

here m_{ms} – mass of the moving parts; x – poppet lift; F_{flow} – flow induced force on the poppet; F_{sp} – spring force; dry friction is neglected due to its small magnitude.

The flow-induced force $F_{\mathrm{flow}} = F_{\mathrm{pr}} + F_{\mathrm{imp}}$ is represented as the sum of a static component F_{pr} and a momentum (reactive) component F_{imp}. Since the momentum component is relatively small compared with the static one, only the static component is considered in the following analysis; for brevity, it will be referred to as the flow force.

To evaluate the flow force F_{pr}, the pressures at the inlet p_{in} and outlet p_{out} of the check valve are used. These pressures are computed as functions of the pressure in the adjacent network node and the liquid mass flow rate through the valve:

$$p_{\mathrm{in}} = p_{\mathrm{n\,i}} - \xi_{\mathrm{in\,i,j}} / \rho \cdot \dot{m}_{\mathrm{i,j}}^2 - J_{\mathrm{in\,i,j}} \frac{d\dot{m}_{\mathrm{i,j}}}{dt}, \tag{7}$$

$$p_{\mathrm{out}} = p_{\mathrm{n\,j}} + \xi_{\mathrm{out\,i,j}} / \rho \cdot \dot{m}_{\mathrm{i,j}}^2 + J_{\mathrm{out\,i,j}} \frac{d\dot{m}_{\mathrm{i,j}}}{dt}, \tag{8}$$

here $p_{\mathrm{n\,i}}$ and $p_{\mathrm{n\,j}}$ – are the pressures i-th and j-th – at the upstream and downstream nodes of the hydraulic network, respectively; $\dot{m}_{\mathrm{i,j}}$ – mass flow in the corresponding pipeline segment; $\xi_{\mathrm{in\,i,j}}$ and $\xi_{\mathrm{out\,i,j}}$ – are hydraulic resistance coefficients of the upstream and downstream segments; $J_{\mathrm{in\,i,j}}$ and $J_{\mathrm{out\,i,j}}$ – are the corresponding inertial resistance coefficients.

Determination of the flow force on the check valve poppet. To determine the pressure distribution over the poppet surface at different valve openings, we performed CFD analysis of the working fluid flow. The calculations were carried out in SOLIDWORKS Flow Simulation using a steady state approach for fixed poppet positions. The geometric model of the flow passage reproduced the critical regions: the valve seat, the sealing element, the clearance between the poppet and the body, and the inlet and outlet ducts.

In the CFD model, the mesh was locally refined in the narrow clearance between the poppet and the seat and in the zone where the jet forms in the annular clearance between the poppet and the body. The minimum cell size was 0.005 mm, and the total number of cells was about 9000000.

The valve walls were stationary with a roughness of 20 μm. The poppet was modeled as a stationary wall fixed at the specified lift. In all runs, the downstream pressure behind the poppet p_2 was held constant at 0.1 MPa.

The CFD solutions yielded pressure and velocity fields in the computational domain for a set of poppet lifts and pressure differentials. Using these data, we obtained the dependence of the flow force F_{pr} on the poppet as a function of lift for different pressure differentials $\Delta p = p_{\text{in}} - p_{\text{out}}$ across the valve. This dependence for $\Delta p = 0.10$ MPa is presented in Fig. 3.

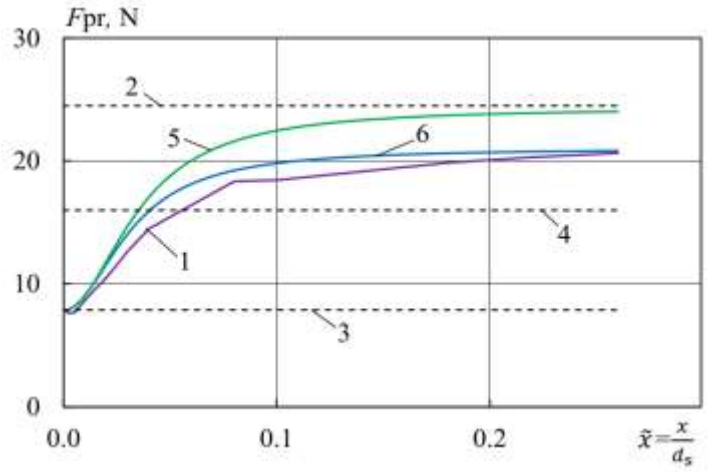

1 – CFD; 2 – $p_{\text{m}} = p_{\text{in}}$; 3 – $p_{\text{m}} = p_{\text{out}}$; 4 – $p_{\text{m}} = \frac{p_{\text{in}} + p_{\text{out}}}{2}$; 5 – p_{m} by equation (12) $a_{10} = 0$ and $a_{20} = 0$; 6 – p_{m} by equation (12) $a_{10} = 0.25\,a_2$ and $a_{20} = 0$

Fig. 3 – Dependence of the static component of the flow-induced force F_{pr} on the valve poppet lift $\tilde{x} = \frac{x}{d_{\text{s}}}$ at $\Delta p = 0.10$ MPa

At small lifts the dominant hydraulic resistance is the narrow throttling clearance between the seat edge and the poppet, and the flow force increases almost linearly with lift. As the valve opens further, the principal throttling element becomes the annular clearance between the poppet and the body, which then accounts for the largest portion of the total pressure drop.

An engineering approximation for the static component of the flow force on the poppet is commonly used [19]:

$$F_{\text{pr}} = (p_{\text{in}} - p_{\text{out}}) \cdot A_{\text{eff}},$$

here p_{in} and p_{out} – inlet and outlet pressures of the check valve; A_{eff} – effective area of the poppet.

In rough estimates A_{eff} is sometimes taken as a constant equal to the seat area or the poppet face area, depending on the design. For higher accuracy, however, A_{eff} must be treated as a function of the pressure differential and of the clearance between the poppet and the seat.

In [20] the flow force is accounted for through a semi empirical lift coefficient expressed as a function of poppet lift c_{f}, which corrects the difference between the actual force F_{flow} and the simple pressure difference force acting on the poppet area

$$F_{\text{flow}} = (p_{\text{in}} - p_{\text{out}}) \cdot f_{\text{s}} \cdot c_{\text{f}}.$$

In [14], the flow-induced force F_{flow} was expressed in the form:

$$F_{\text{flow}} = \alpha(p_{\text{in}} + \rho \cdot u_1^2 / 2) + \gamma(p_{\text{out}} + \rho \cdot u_2^2 / 2) + \beta \dot{m},$$

where α and γ – coefficients have units of area and represent the effective poppet area on the inlet and outlet sides, respectively; β – coefficient accounts for the flow velocity in the clearance. These coefficients are obtained from CFD calculations.

To capture the pressure non uniformity more accurately, we apply a split surface approach that accounts separately for the pressures acting on different parts of the poppet. For the present valve, using the computational scheme in Fig. 2, the flow force F_{pr} can be written in the form:

$$F_{\text{pr}} = p_{\text{in}} \cdot A_{\text{s}} + p_{\text{m}} \cdot (A_{\text{p}} - A_{\text{s}}) - p_{\text{out}} \cdot A_{\text{p}}, \quad (9)$$

where A_{s} – seat area, $A_{\text{s}} = \pi \cdot d_{\text{s}}^2 / 4$; A_{p} – poppet face area, $A_{\text{p}} = \pi \cdot d_{\text{p}}^2 / 4$; d_{p} – poppet diameter; p_{m} – pressure in the annular cavity A bounded by the area $(A_{\text{p}} - A_{\text{s}})$.

If, in (9), one sets $p_{\text{m}} = p_{\text{out}}$, the resulting flow-induced force F_{pr} becomes constant, which fails to reflect its variation from the CFD results (see curve 2 in Fig. 3). A similar outcome occurs for $p_{\text{m}} = p_{\text{out}}$ or $p_{\text{m}} = \frac{p_{\text{in}} + p_{\text{out}}}{2}$ (see curves 3 and 4 in Fig. 3).

To reconcile the force F_{pr} computed by equation (9) with the CFD results, the flow passage of the check valve from inlet to outlet is split into two segments. Neglecting the compliance of cavity A, the momentum equations for these segments are written as:

$$p_{\text{in}} = p_{\text{m}} + (a_{10} + a_1)\dot{m}_1^2, \quad (10)$$

$$p_{\text{m}} = p_{\text{out}} + (a_{20} + a_2)\dot{m}_2^2, \quad (11)$$

where a_1, a_2 – pressure-loss coefficients determined by the minimum effective flow areas on the segments

$$a_1 = \frac{1}{2\rho(\mu_1 A_1)^2}, \quad a_2 = \frac{1}{2\rho(\mu_2 A_2)^2};$$

A_1, μ_1 – are the area and the discharge coefficient of the annular clearance between the poppet and the seat

$$A_1 = \pi \cdot d_s \cdot x;$$

A_2, μ_2 – are the area and the discharge coefficient of the radial clearance between the body and the poppet

$$A_2 = \pi \cdot (d_b^2 - d_p^2)/4,$$

d_b – is the inner body diameter; a_{10}, a_{20} – additional pressure-loss coefficients accounting for turning, local, and friction losses (unlike a_1 and a_2); $\dot{m}_1$, $\dot{m}_2$ – mass flows in segments 1 and 2.

Assuming $\dot{m}_1 = \dot{m}_2$, (10) and (11) yield an expression for the pressure in cavity A in terms of p_m:

$$p_m = \frac{p_{in}\left(a_{20} + \frac{1}{2\rho(\mu_2 A_2)^2}\right) + p_{out}\left(a_{10} + \frac{1}{2\rho(\mu_1 A_1)^2}\right)}{a_{10} + \frac{1}{2\rho(\mu_1 A_1)^2} + a_{20} + \frac{1}{2\rho(\mu_2 A_2)^2}}. \qquad (12)$$

Using p_m from equation (12) to compute F_{pr} with $a_{10} = 0$ and $a_{20} = 0$ produces the curve in Fig. 3 (curve 5), which reproduces the qualitative increase of F_{pr} with poppet lift observed in the CFD results. Including additional pressure losses on the first segment $a_{10} \neq 0$ yields satisfactory quantitative agreement between the predictions of equations (9) and (12) and the CFD results; this is illustrated by curve 6 in Fig. 3 (obtained for representative values of $a_{10} = 0.25 a_2$ relative to the segment-loss terms).

Satisfactory agreement for F_{pr} was also obtained for other pressure differentials across the check valve (see Fig. 4).

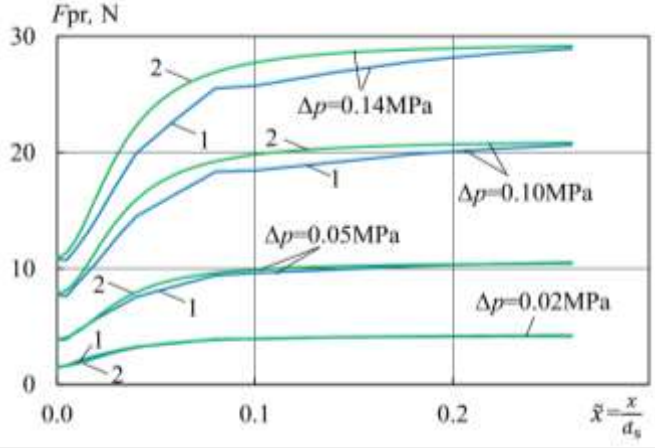

1 – CFD; 2 – p_m by equation (12) for $a_{10} = 0.25\, a_2$ and $a_{20} = 0$

Fig. 4 – Dependence of the flow force F_{pr} on poppet lift $\tilde{x} = \frac{x}{d_s}$

4. Results of transient simulations. For the transient simulations of the LPRE gas generator feed system, the boundary conditions were: a constant pressure in the starting tank p_B, the oxidizer flow rate to the gas generator $\dot{m}_{ogg}$, and the fuel pump discharge pressure p_p. The increases in oxidizer flow rate and in pump discharge pressure were prescribed as linear functions of time, which reflects the physics of start up: a progressively increasing oxidizer supply and a gradual pressure rise in the pump line as the turbine spins up.

Transient calculations for the variable structure fuel feed system during engine start were performed using the mathematical model (1) – (8). In this model, the flow induced force acting on the check valve poppet, F_{pr}, was either taken from CFD analysis or approximated by the lumped parameter method using equations (9), (12).

At the initial stage of start, fuel is supplied to the gas generator only from the starting tank and reaches its maximum values. This occurs because there is no counter pressure in the gas generator. After ignition in the gas generator and turbine spin up, the pressure behind the pump begins to rise. When the pump discharge pressure reaches a certain level, the fuel feed switches to the pump. This switching is automatic and is performed by check valves 1 and 2.

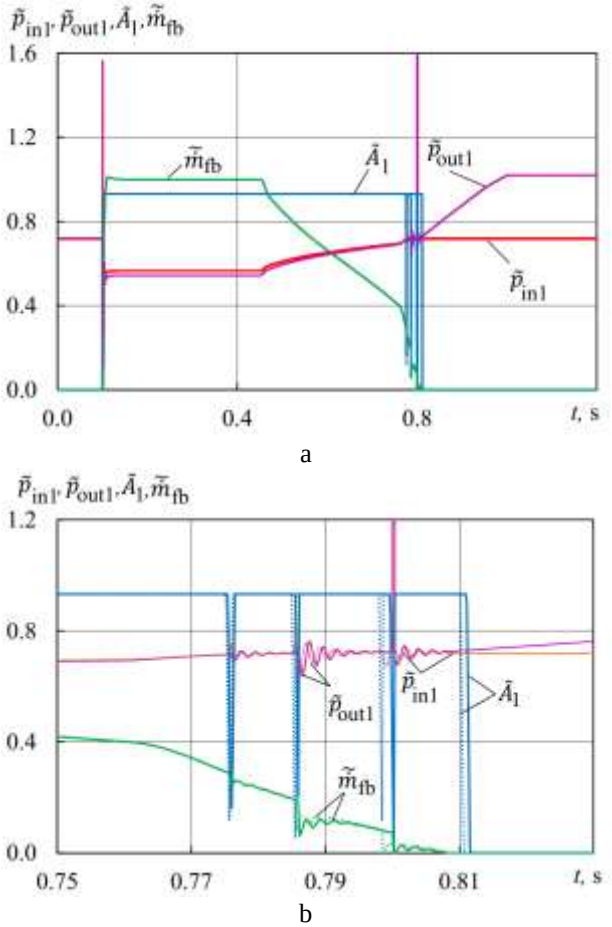

a – time window 0–1.2 s; b – time window 0.75–0.83 s; solid lines – flow force F_{pr} from CFD; dashed lines – flow force F_{pr} from equations (9), (12)

Fig. 5 – Evolution of check valve 1 parameters during LPRE start up

Figures 5 and 6 show the operating characteristics of the check valves during start up: time histories of the relative fuel mass flows ($\tilde{m}_{\text{fp}}$, $\tilde{m}_{\text{fb}}$), the relative inlet pressures ($\tilde{p}_{\text{in1}}$, $\tilde{p}_{\text{in2}}$) and outlet pressures ($\tilde{p}_{\text{out1}}$, $\tilde{p}_{\text{out2}}$) of the check valves, and the relative effective flow areas ($\tilde{A}_1$, $\tilde{A}_2$) of the valves (normalized by their maximum values). Relative flow values were defined as the ratio of the current fuel flow to the maximum fuel flow in the gas generator. The reference pressure level was the gas generator pressure at the nominal operating point.

Analysis of Figs. 5 and 6 indicates that closing of valve 1 and opening of valve 2 begin simultaneously at 0.76 s. This is accompanied by a decrease of the flow through valve 1 and an increase through valve 2. The opening of valve 2 under a steadily rising pump discharge pressure proceeds monotonically, without poppet oscillations (see Fig. 6). In contrast, the closing of valve 1 under the action of backpressure p_1 is non monotonic and is accompanied by oscillations of the poppet lift (see Fig. 5). This behavior of valve 1 lift is caused by the fact that partial throttling and flow reduction through the valve lowers the pressure at p_1. The drop can be sufficient to drive the poppet toward reopening. For valve 1 these conditions occur at 0.776 s, 0.786 s, and 0.800 s. Fast chattering of the valve 1 poppet produces local disturbances and transients not only in the branch of valve 1 but in the entire hydraulic system.

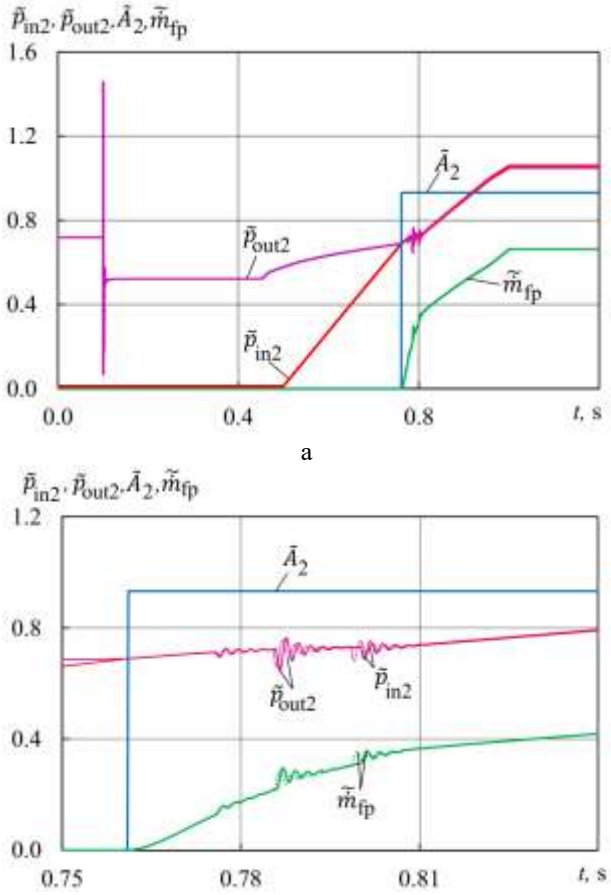

a – time window 0–1.2 s; b – time window 0.75–0.83 s; solid lines – flow force F_{pr} from CFD; dashed lines – flow force F_{pr} from equations (9), (12)

Fig. 6 – Evolution of check valve 2 parameters during LPRE start up

The transient simulation results obtained using CFD based flow forces and those using the lumped parameter approximation agree well overall. A difference is observed for the force F_{pr} on the poppet of valve 1, which leads to different actuation times. The largest difference in the onset time of actuation, corresponding to complete closure of the valve, does not exceed 0.0021 s.

The proposed lumped parameter method for approximating the flow induced forces on the poppets of check valves enables the development of mathematical models of variable structure hydraulic systems and transient analyses with sufficient accuracy without resorting to costly CFD calculation.

Conclusions.

1. An approach is proposed for determining the flow induced force on a check valve poppet using a lumped parameter approximation based on a balance of the working fluid flow rates in the valve passage. The model considers a radial inflow at the valve inlet, which depends on poppet lift, and the peripheral flow in the narrow clearance between the body and the poppet. To apply this approach, it is sufficient to know the geometric parameters of the valve and to use discharge coefficients taken as constants.

2. For a variable structure fuel feed hydraulic system containing check valves, a low frequency mathematical model of the dynamic processes was developed, and transient calculations were performed for LPRE start up. During start up, the gas generator fuel feed automatically switches from the starting tank to the pump via the action of check valves. Transients were computed for two variants of the flow force model on the check valve poppet: one based on CFD analysis and one based on the lumped parameter approximation. The two approaches showed satisfactory agreement.

3. The feasibility of using the proposed lumped parameter approximation for the flow induced force on a check valve poppet has been substantiated for constructing mathematical models of dynamic processes in variable structure hydraulic systems without the need for labor intensive CFD calculations.

1. *Sutton G. P., Biblarz O.* Rocket Propulsion Elements. 9-te ed. Hoboken: John Wiley & Sons, 2017. 800 p.
2. *Huze, D. K., Huang D. H.* Design of Liquid Propellant Rocket Engines. NASA SP-125. Washington: NASA, 1971. 472 p.
3. *Cherniavskyi O., Shevchenko S., Dolgopolov S.* Mathematical modeling of the dynamic processes during check valve operation in the branched reconfigurable feed system of a liquid rocket engine. Aerospace engineering and technology. 2025. No. 4, special issue 2, (206). P. 93–101.
4. *Pylypenko O., Dolgopolov S., Nikolayev O., Khoriak N., Kvasha Yu., Bashliy I.* Determination of the thrust spread in the Cyclone-4M first stage multi-engine propulsion system during its start. Science and Innovation. 2022. Vol. 18, № 6. P. 97–112.
5. *Koptilyy D., Marchan R., Dolgopolov S., Nikolayev O.* Mathematical modeling of transient processes during start-up of main liquid propellant engine under hot test conditions. Proceedings of the 8th European Conference on Aeronautics and Space Sciences (EUCASS), Madrid, Spain, 1–4 July. 2019. 15 p.
6. *Kobielski M. J., Skarka W., Skarka M.* Comparison of pressure-loss evaluation fidelity in turbulent energy dissipation models of poppet check valves using computational fluid dynamics (CFD) software. Technical Sciences. 2024. Vol. 27. P. 19–31. https://doi.org/10.31648/ts.9732
7. *Filo G., Lisowski E., Rajda J.* Design and Flow Analysis of an Adjustable Check Valve by Means of CFD Method. Energies. 2021. Vol, 14. No. 8. P.2237. https://doi.org/10.3390/en14082237
8. *Klas R., Habán V., Rudolf P.* Analysis of in-line check valve with respect to the pipeline dynamics. EPJ Web of Conferences. 2017. Vol. 143. P. 02051. https://doi.org/10.1051/epjconf/201714302051
9. *Lang S.* A review of check valves in unsteady flow. Proceedings of the 2024 ASME Pressure Vessels & Piping Conference, V003T04A001.
10. *Domagała M., Fabis-Domagała J. A* Review of the CFD Method in the Modeling of Flow Forces. Energies. 2023. Vol 16, No. 16. P. 6059. https://doi.org/10.3390/en16166059
11. *Pusztai T., Siménfalvi Z.* CFD analysis on a direct spring-loaded safety valve to determine flow forces. Pollack Periodica. 2021. Vol.16. No.1. Pp. 109–113. https://doi.org/10.1556/606.2020.00122
12. *Zong C., Zheng F., Chen D., Dempster W., Song X.* CFD Analysis of the Flow Force Exerted On the Disc of a Direct-Operated Pressure Safety Valve in Energy System. Journal of Pressure Vessel Technology. 2020. Vol.142, No.1. P.011702. https://doi.org/10.1115/1.4045131
13. *Finesso R., Rundo M.* Numerical and experimental investigation on a conical poppet relief valve with flow force compensation. International Journal of Fluid Power. 2017. Vol. 18, No. 2. Pp. 111–122. https://doi.org/10.1080/14399776.2017.1296740

14. *Wu D., L, S., Wu P.* CFD simulation of flow-pressure characteristics of a pressure control valve for automotive fuel supply system. Energy Conversion and Management. 2015. Vol. 101. P. 410–419. https://doi.org/10.1016/j.enconman.2015.06.025
15. *Lisowski E., Rajda J.* Analysis of the Design of a Poppet Valve by Transitory Simulation. Energies. 2019. Vol. 12, No. 5. P. 889. https://doi.org/10.3390/en12050889
16. *Marchan R. A.* Small-scale supersonic combustion chamber with a gas-dynamic ignition system. Combustion Science and Technology. 2011. Vol. 183, № 11. P. 1236–1265. https://doi.org/10.1080/00102202.2011.589874
17. *Marchan R., Oleshchenko A., Vekilov S., Arsenuk M., Bobrov O.* 3D printed acoustic igniter of oxygen-kerosene mixtures for aerospace applications. Proceedings of the 8th European Conference on Aeronautics and Space Sciences (EUCASS), Madrid, Spain, 1–4 July. 2019. 14 p.
18. *Raman G., Srinivasan K.* The powered resonance tube: From Hartmann's discovery to current active flow control applications. Progress in Aerospace Sciences. 2009. Vol. 45, No. 4-5. P. 97–123. https://doi.org/10.1016/j.paerosci.2009.05.001
19. *Guillon M.* Hydraulic servo systems: Analysis and design. Butterworth, 1969. 462 p.
20. *Habing R. A., Peters M.C.A.M.* An experimental method for validating compressor valve vibration theory. Journal of Fluids and Structures. 2006. Vol. 22, No. 5. P. 683–697. https://doi.org/10.1016/j.jfluidstructs.2006.03.003

Received on October 22, 2025,
in final form on December 1, 2025